HHS Public Access

Author manuscript

Chem Res Toxicol. Author manuscript; available in PMC 2022 May 17.

Benzalkonium chloride disinfectants induce apoptosis, inhibit proliferation, and activate the integrated stress response in a 3-D *in vitro* model of neurodevelopment

Josi M. Herron[†,‡], **Hideaki Tomita**[‡], **Collin C. White**[†], **Terrance J. Kavanagh**[†], **Libin Xu**[†,‡,*]

[†]Department of Environmental and Occupational Health Sciences, University of Washington, Seattle, WA

[‡]Department of Medicinal Chemistry, University of Washington, Seattle, WA

Abstract

We previously found that the widely used disinfectants, benzalkonium chlorides (BACs), alter cholesterol and lipid homeostasis in neuronal cell lines and in neonatal mouse brains. Here we investigate the effects of BACs on neurospheres, an *in vitro* three-dimensional model of neurodevelopment. Neurospheres cultured from mouse embryonic neural progenitor cells (NPCs) were exposed to increasing concentrations (1 to 100 nM) of a short-chain BAC (BAC C12), a long-chain BAC (BAC C16), and AY9944 (a known DHCR7 inhibitor). We found that the sizes of neurospheres were decreased by both BACs, but not by AY9944. Furthermore, we observed potent inhibition of cholesterol biosynthesis at the step of DHCR7 by BAC C12, but not by BAC C16, suggesting that cholesterol biosynthesis inhibition is not responsible for the observed reduction in neurosphere growth. Using immunostaining and cell cycle analysis, we found that both BACs induced apoptosis and decreased proliferation of NPCs. To explore the mechanisms underlying their effect on neurosphere growth, we carried out RNA sequencing on neurospheres exposed to each BAC at 50 nM for 24 hr, which revealed activation of the integrated stress response by both BACs. Overall, these results suggest that BACs affect neurodevelopment by inducing the integrated stress response in a manner independent of their effects on cholesterol biosynthesis.

Graphical Abstract

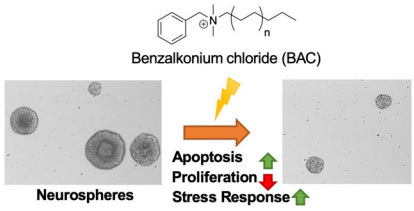

[*]Corresponding author: Libin Xu, Ph.D., libinxu@uw.edu, Phone: (206) 543-1080, Fax: (206) 685-3252.

Author contributions

JH and LX designed the study; JH, HT, and CW conducted the experiments; JH, CCW, and LX analyzed the data; JH and LX drafted the manuscript with contribution from all authors.

Keywords

benzalkonium chloride; neurosphere; apoptosis; cholesterol biosynthesis; integrated stress response

Introduction

Benzalkonium chlorides (BACs) are the most commonly used quaternary ammonium compound (QAC) disinfectants. They are applied in food processing lines, health care facilities, residential settings, and are common ingredients in over-the-counter cosmetics, hand sanitizers, and pharmaceutical products.[1, 2] Therefore, exposure to BACs is prevalent given the diversity of applications and may occur through dermal/eye contact, inhalation, and ingestion. The COVID-19 pandemic has led to excessive usage of BAC-containing disinfectants. Clorox has ramped up its production by 5 times but still cannot meet the demand. Thus, the level of exposure to BACs is unprecedented. Although BACs have been generally recognized as safe, the FDA has called for additional safety data on the usage of BACs in healthcare and consumer antiseptic products.[3, 4]

A wide range of cytotoxicity and biological activities of BACs has been reported in various biological systems. Occupational BAC exposure has been found to be associated with increased risk of asthma and allergic reactions in the eye and the skin.[5–10] BACs are toxic to peripheral neurons, including enteric and ganglion neuronal cells, at μM concentrations.[11, 12] A study by Hrubec and coworkers demonstrated that chronic consumption of BACs-containing diet led to significantly decreased fertility and fecundity in mice, as well as increased dam mortality.[13] Recently, the same group reported an increased incidence of neural tube defects (NTDs) in both mice and rats exposed *in utero*, either through diet or ambiently, to an environmentally relevant QAC mixture that contained BACs.[14] NTDs are closely associated with defects in neural progenitor cell (NPC) proliferation.[15–17] Indeed, rat NPCs exposed to high concentrations (1000 nM) of BACs *in vitro* show decreased proliferation, increased apoptosis, and oxidative stress.[18]

We previously found that BACs with short alkyl chains, C10 or C12, inhibit cholesterol biosynthesis at the step of 7-dehydrocholesterol reductase (DHCR7) in Neuro2a cells.[19] Recently, we demonstrated that BACs accumulate in the developing neonatal mouse brain at low nM concentrations and alter cholesterol biosynthesis.[20] Cholesterol is critical for neurodevelopment, serving an essential role in hedgehog signaling,[21] neurogenesis,[22] synapse formation and function,[23, 24] and myelination.[25] Effects on cholesterol homeostasis have been shown to play a role in the developmental neurotoxicity of ethanol and retinoic acid.[26, 27] Therefore, it is plausible that BACs may impact neurodevelopment in a manner similar to these well-known developmental neurotoxicants.

Neurospheres are used as a three-dimensional (3-D) *in vitro* model for developmental neurotoxicity screening as they mimic key processes of brain development, including proliferation, apoptosis, differentiation, and migration.[28, 29] Neurospheres are free-floating structures consisting of NPCs. In the present study, we found that BACs increase apoptosis

and decrease proliferation of neurospheres in a manner that is associated with induction of the integrated stress response rather than cholesterol biosynthesis inhibition.

Materials and Methods

Materials

Optima LC/MS solvents (chloroform, methanol, methylene chloride, and water), formic acid (Optima LC/MS), and sodium chloride were purchased from Thermo Fisher Scientific (Grand Island, NY). Benzyldimethyldodecylammonium chloride (BAC C12) and benzyldimethylhexadecylammonium chloride (BAC C16) were purchased from Sigma-Aldrich Co. (St. Louis, MO). BAC C12 and BAC C16 were dissolved in DMSO to yield 1, 10, 50, and 100 μM stocks and stored at −80°C. The deuterated (d_7-) sterol standard d_7-7-dehydrocholesterol was prepared as reported previously.[30] d_7-Cholesterol was purchased from Avanti Polar Lipids (Alabaster, AL). $^{13}C_3$-desmosterol and $^{13}C_3$-lanosterol were purchased from Kerafast (Boston, MA). The primary antibody used in immunocytochemistry was mouse anti-Ki67 at a dilution of 1:200 (BD Pharmingen™, San Jose, CA) and the secondary antibody used was Alexa Fluor-conjugated goat anti-mouse IgG at a dilution of 1:1000 (Invitrogen ™, Carlsbad, CA). 4,6-Diamidino-2-phenylindole (DAPI) was purchased from Thermo Fisher Scientific.

Cell culture

The University of Washington Institutional Animal Care and Use Committee approved all animal protocols. Male and female C57BL/6J mice (7 to 8 weeks old) were purchased from Jackson Laboratories (Bar Harbor, ME). Time-mating was conducted with breeding pairs of 2 females and one male, placed in a cage overnight and separated the following morning. On gestation day 13.5 to 14.5, the pregnant dam was euthanized, and embryos were removed from the uterus and transferred to a Petri dish in sterile 1x phosphate buffered saline (PBS). After careful removal of the meninges under a dissection microscope, cortices were dissected from each embryo, and transferred to a 60 mm culture dish containing 1 to 2 mL of neurosphere proliferation media [DMEM/F-12 medium (Gibco®, Grand Island, NY), Non-Essential Amino Acids (1x; Gibco®), GlutaMax (1x; Gibco®), Penicillin (100 IU) plus Streptomycin (100 μg/mL) Strep (Gibco®), Sodium Pyruvate (1x; Gibco®), B27 (1x; Gibco®), 20 ng/mL basic fibroblast growth factor (bFGF) and 20 ng/mL epidermal growth factor (EGF) (PeproTech®, Rocky Hill, NJ)]. Tissues in media were transferred to a 15 mL conical falcon tube and gently dissociated by trituration until clumps were no longer visible. Cells were filtered through a 40 μm sterile cell strainer, seeded in neurosphere proliferation media at either a density of 30,000 cells per well in 6-well plates for sterols analysis, immunocytochemistry, transcriptomics, and flow cytometry experiments, or a density of 3,000 cells per well in a flat-bottom, ultra-low attachment 96-well plate (Corning™, Corning, NY) for growth analysis, and cultured at 37 °C and 5% CO_2/ 95% humidified air. After 2 to 3 days, small neurospheres were formed, with peak neurosphere formation occurring at 5 to 7 days when neurospheres reached approximately 150 to 200 μm in diameter. Each preparation of neurospheres was considered one biological replicate and a minimum of 3 replicates were used for each experiment.

Chemical treatment

Neurospheres were exposed to BAC C12, BAC C16, AY9944 (the positive control for cholesterol biosynthesis inhibition) or vehicle control (0.1% DMSO) from day *in vitro* 4 (DIV 4) to DIV 7 for sterols analysis, growth analysis, and immunocytochemistry. For transcriptomic analyses and flow cytometry, neurospheres were exposed from DIV 4 to DIV 5. Concentrations are described in figures and figure legends.

Neurosphere growth analysis

Neurosphere growth was evaluated at DIV 7 after exposure to BACs, AY9944 or vehicle control in triplicate wells of a 96-well plate. Brightfield images of neurospheres were captured on an EVOS® FL Auto Imaging System (Thermo Fisher Scientific) using the 10x objective. ImageJ processing and analysis software (NIH) was used to measure the diameter of each neurosphere in each of 3 wells per condition. Only neurospheres greater than 40 μm in diameter were measured. Data are presented as box plots, with individual data-points representing each neurosphere. Statistical analyses were conducted using ANOVA followed by Dunnett's test comparing multiple concentrations to a single control, with an adjusted P value < 0.05 considered statistically significant (GraphPad Prism version 9 for Windows).

To evaluate cell count on DIV 7, neurospheres were collected from triplicate wells of a 6-well plate and mechanically dissociated into a single cell suspension for each condition. An aliquot of cell suspension was used for counting and the remaining cell suspension was used for immunocytochemistry. Data are presented as mean ± standard error of the mean. Statistical analyses were conducted as described above.

Sterols analysis

On DIV 7, neurospheres exposed to BAC C12, BAC C16, or vehicle control in triplicate wells of a 6-well plate were pelleted and sonicated in ice cold 100 μL 1x PBS to lyse them. Protein mass was measured with the BioRad-DC Protein Assay Kit. Isotopically labeled sterol internal standards (to be used for quantification in the sterols analysis) were added to each neurosphere lysates as follows: 0.5 μg of d_7-cholesterol and d_7-7-dehydrocholesterol, and 0.1 μg of $^{13}C_3$-lanosterol and $^{13}C_3$-desmosterol. Lipid extraction was carried out as previously described in detail.[31] To extract the lipids, Folch solution [4 mL chloroform/methanol (2/1, v/v)] and NaCl aqueous solutions (0.9% (w/v), 1 mL) were added to each cell lysate sample and the mixture was briefly vortexed and then centrifuged for 5 min in a clinical tabletop centrifuge at 10°C. The lower (organic) phase was recovered, transferred to a separate glass tube, and the solvent was removed *in vacuo* using a SpeedVac® (Thermo Fisher Savant). The resulting lipid extracts were re-dissolved in 0.3 mL methylene chloride prior to analysis.

For analysis, 30 μL of lipid extract was transferred to an LC vial, dried under a stream of argon, and reconstituted in 30 μL 90% MeOH with 0.1% formic acid. Determination of sterol concentrations was performed by ultra-performance liquid chromatography (UPLC) tandem mass spectrometry (MS/MS) using a triple-quadrupole mass spectrometer (API 4000 ™; AB SCIEX, Ontario, Canada) equipped with atmospheric pressure chemical ionization (APCI) coupled to a Waters Acquity UPLC system as described previously.31 Briefly,

sterols were separated by reversed phase chromatography on a C18 column (1.7 mm, 2.1 × 100 mm, Phenomenex Kinetex) using a 15 min isocratic gradient of 90% methanol with 0.1% formic acid at a flow of 0.4 mL/min. Selective reaction monitoring (SRM) was used to monitor the dehydration of the sterol [M+H]+ ions to generate [M+H-H_2O]+ ions. Data analysis was performed with Analyst (v. 1.6.2) Quantitation Wizard. Cholesterol was quantified relative to the d_7-cholesterol internal standard, 7-dehydrocholesterol and 8-dehydrocholesterol was quantified relative to d_7-7-dehydrocholesterol, 7-dehydrodesomsterol and desmosterol were quantified relative to $^{13}C_3$-desmosterol, and lanosterol was quantified relative to $^{13}C_3$-lanosterol. Data are presented as mean ± standard deviation. Statistical analyses were conducted using ANOVA followed by Dunnett's test comparing multiple concentrations to a single control, with an adjusted P value < 0.05 considered statistically significant (GraphPad Prism version 9 for Windows).

Immunocytochemistry

For determination of cell proliferation by immunocytochemistry, 5-ethynyl-2'-deoxyuridine (EdU) was added to each well at a final concentration of 10 μM 4 hrs before the end of treatment to label cells undergoing proliferation. Neurospheres exposed to BAC C12, BAC C16, or vehicle control in triplicate wells of a 6-well plate were then collected into a pellet and triturated into a single cell suspension of NPCs. NPCs were seeded in untreated neurosphere proliferation medium at a density of 100,000 cells per well in a 4-well Permanox™ plastic chamber slide (Nunc™, Thermo Fisher Scientific) freshly coated with poly-d-lysine (20 μg/mL; Sigma Aldrich) and laminin (2 μg/mL; Corning™, Corning, NY). Cells were left to adhere overnight in the incubator and then fixed with 4% paraformaldehyde (PFA) in PBS for 20 min at room temperature. PFA was aspirated and cells were washed 3 × 5 min with 1x PBS. For immunocytochemistry, the PBS was aspirated, and cells were permeabilized with 3% BSA in PBST (0.5% Triton-X 100 in PBS) for 20 min at RT.

For evaluation of proliferation, fixed cells were first exposed to 10% goat serum in PBST for 1 hr at room temperature and then exposed to Ki67 (1:200) and 5% goat serum in PBST overnight at 4°. Cells were washed with cold PBST for 5 × 5 min. Alexa 568 goat anti-mouse secondary antibody was applied for 1 hr at RT and then cells were washed with cold PBST for 5 × 10 min. After the 4th wash, cells were incubated with 1 μg/mL DAPI for 20 min and washed once again with PBST. Coverslips were applied using Aqua Poly/Mount (Polysciences, Warrington, PA). For EdU staining, the cells underwent an additional processing step prior to blocking per the manufacturer's protocol (MP 10338, Click-iT® EdU Imaging Kit, Thermo Fisher Scientific). For evaluation of apoptosis, cells on slides separate from those used for proliferation analysis were washed in PBS for 5 min at room temperature and permeabilized in PBST for 5 min. Cells were rinsed with PBS for 2 × 5 min at room temperature. Excess liquid was removed and the TUNEL reaction was conducted per manufacturer's protocol (#TB235, DeadEnd™ Fluorometric TUNEL System, Promega). DAPI incubation was conducted as described above followed by application of coverslips using Aqua Poly/Mount.

Fluorescent images of NPCs were captured on an EVOS® FL Auto Imaging System (Thermo Fisher Scientific) using the 20x objective. Images were uniformly adjusted for brightness and contrast. A cell was scored as marker-positive if the cell showed positive staining for DAPI and the marker. A cell with nuclear condensation was scored as apoptotic. At least 500 DAPI-positive cells per condition per biological replicate were quantified and the experimenter was blinded to condition. Data are presented as mean ± standard error of the mean. Statistical analyses were conducted as described above.

Flow cytometry analysis of cell cycle

Following exposure to vehicle control (DMSO), AY9944, BAC C12, or BAC C16 for 24 hr at 50 nM, neurospheres were pelleted and the supernatant was aspirated. The pellet was resuspended in 500 μl of 10 μg/ml DAPI and 0.1% IGEPAL CA-630 detergent (Sigma I8896) in Tris buffered saline. To lyse cells and release intact nuclei, the pellet was triturated using a 1 mL syringe with a 25-gauge needle. Isolated nuclei were filtered through a 37 μm steel mesh fitted onto a pipette tip. The nuclei suspension was analyzed using a BD™ LSR II cytometer with ultraviolet excitation and DAPI emission collected at > 450 nm. Cell cycle was analyzed using the software program FlowJo™. Data are presented as mean ± standard error of the mean. Statistical analyses were conducted using paired Student's t-test with a P value < 0.05 considered statistically significant (Microsoft Excel).

Transcriptomics analysis

Neurospheres exposed to BAC C12, BAC C16, or vehicle control from DIV 4 to DIV 5 in 4 wells of a 6-well plate were pelleted. Pellets (n = 3 biological replicates per condition) were homogenized in 1 mL of QIAzol Lysis Reagent (Qiagen, Germantown, MD). Total RNA was extracted from each sample using the RNeasy Mini Kit (Qiagen) according to the manufacturer's protocol. RNA concentration was quantified using a microplate spectrophotometer (Bio-Tek, Winooski, VT) to quantify the absorbance at 260 nm. RNA integrity was evaluated by formaldehyde agarose gel electrophoresis to visualize the 18S and 28S rRNA bands. RNA integrity and purity were further confirmed by Novogene (Chula Vista, CA) using an Agilent 2100 BioAnalyzer (Agilent Technologies Inc., Santa Clara, California). Samples with RNA Integrity Number (RIN) of 10.0 or above were submitted for RNA sequencing. Novogene performed the cDNA library construction and sequencing using the Illumina NovaSeq 6000 platform (150 base pairs paired-end, with sequencing depth above 20 million reads per sample).

Raw RNA sequencing reads in FASTQ format were mapped to the mouse genome using HISAT (https://ccb.jhu.edu/software/hisat/index.shtml; Last accessed 8/31/2020) and format conversions were performed using Samtools. Cufflinks (http://cufflinks.cbcb.umd.edu/; Last accessed 8/31/2020) was used to estimate relative abundances of transcripts from each RNA sample. Cuffdiff, a module of Cufflinks, was used to determine differentially expressed genes (DEGs) between control and BAC C12, as well as control and BAC C16. DEGs met the criterion of an adjusted P value < 0.05 (corresponding to the allowed false discovery rate of 5%). DEGs were plotted in a Venn diagram to identify common and uniquely expressed genes for each condition. Analysis of gene ontology (GO) terms for biological processes was performed using iPathwayGuide (Advaita). DEGs were also submitted for STRING

(Search Tool for the Retrieval of Interacting Genes/Proteins) analysis (https://string-db.org/; Last accessed 08/31/2020). Transcriptomic data is publicly available at DRYAD (https://doi.org/10.5061/dryad.v6wwpzgv5) and Table S2.

Results

Neurosphere growth is reduced by BACs

We first aimed to establish the phenotype of neurosphere growth in the presence of BACs. Alterations in neurosphere growth could indicate increased cell death and/or an impairment in the ability of NPCs to proliferate. Therefore, effects on the growth of neurospheres exposed to either BAC C12, BAC C16, or AY9944 (the positive control for cholesterol biosynthesis inhibition), from DIV 4 to DIV 7 was investigated. We chose to use BAC C12 and C16 to cover the full spectrum of biological actions of BACs because BAC C12 has been found to be a potent inhibitor of DHCR7 while BAC C16 exhibit more potent cytotoxicity in Neuro2a cells.[19] Neurospheres exposed to either BAC showed a significant decrease in diameter compared to vehicle control exposed neurospheres (Figure 1A–B). The decrease in diameter was correlated with a reduction in the number of cells obtained from dissociated neurospheres (Figure 1C). However, AY9944, a known inhibitor of DHCR7, did not cause significant changes in the neurosphere growth and cell count.

BACs alter cholesterol biosynthesis in neurospheres

Previously, we found that treatment of neurospheres with AY9944 resulted in increased levels of cholesterol precursors, 7-dehydrocholesterol (7-DHC) and 7-dehydrodesmosterol (7-DHD), and decreased levels of desmosterol and cholesterol – alterations that are expected in the event of pathway inhibition at the step of DHCR7 (Figure S1).[31] In the current study, neurospheres were exposed to low nM concentrations of BACs from DIV4 to DIV7 and UHPLC-MS/MS analysis was conducted to quantify levels of sterols in the post-squalene cholesterol biosynthetic pathway (Figure 2).

Decreased desmosterol levels were observed at 50 nM in BAC C12 exposed neurospheres and at 100 nM in BAC C16 exposed neurospheres. A trend toward decreased cholesterol and lanosterol levels was also observed in BAC-exposed neurospheres, although this was not statistically significant. The cholesterol precursors, 7-DHC and 7-DHD, were significantly increased in neurospheres exposed to BAC C12 at 50 nM. 8-Dehdyrocholesterol also showed significant accumulation in neurospheres exposed to 100 nM BAC C12. Overall, the effect of BAC C12 on sterol levels in neurospheres is consistent with the inhibition of DHCR7 in the cholesterol biosynthetic pathway and our previous observations.[19, 31] BAC C16 is much less potent than BAC C12 in inhibiting cholesterol biosynthesis. Regardless, these effects do not appear to be correlated with effects on neurosphere growth, as both BACs decreased neurosphere diameter and cell count and AY9944, a known and potent inhibitor of cholesterol biosynthesis, did not.

BACs decrease proliferation and induce apoptosis

The observed reduction in neurosphere growth could be due to decreased proliferation and/or increased apoptosis of the NPCs. To evaluate the effects of BACs on proliferation,

Ki67, a widely accepted cell proliferation marker, and EdU, a thymidine analog that is incorporated into DNA of proliferating cells, were used to assess the number of proliferating cells and proliferation rate (% EdU-positive cells / Ki67-positive cells). We found that the total number of Ki67-positive cells from BAC-exposed neurospheres was decreased although the proliferation rate was not affected (Figure 3A–B). Furthermore, cell cycle analysis using flow cytometry revealed an apparent delay of the G1/S phase transition, demonstrated by a significant increase in G1 cells and corresponding decrease in S phase cells from BAC C12 exposed neurospheres (Figure 3C). This trend was the same for BAC C16 exposed neurospheres, although not statistically significant due to large variation between biological replicates.

To evaluate the effects of BACs on apoptosis, the terminal deoxynucleotidyl transferase (TdT) dUTP nick-end labeling (TUNEL) assay and the condensed nuclei assay were used to quantify apoptotic cells. After the neurospheres were exposed to BACs from DIV 4 to DIV 7, an increase in the number of TUNEL-positive NPCs (Figure 4A–B) and condensed nuclei (Figure 4C–D) from dissociated neurospheres were observed. Collectively, these results suggest that the reduction in neurosphere growth was due to both a decrease in proliferation and increase in apoptosis.

Transcriptome analysis identified biological processes affected by BACs

As discussed above, the effects of BACs on neurosphere growth do not correlate with their effects on cholesterol biosynthesis. Therefore, to determine potential mechanisms underlying the effects of BACs on neurosphere growth, global transcriptomic analysis was conducted on neurospheres exposed to BACs from DIV 4 to DIV 5. We identified 116 differentially expressed genes (DEGs) from BAC C12-exposed neurospheres (adjusted P value < 0.05; Figure 5A) and 37 DEGs from BAC C16-exposed neurospheres. BAC C12 and BAC C16 co-regulated 9 genes (Figure 5A).

Functional characterization of DEGs was conducted using gene ontology (GO) analysis of biological processes. GO analysis identified 1,143 biological processes significantly enriched by BAC C12, 445 significantly enriched by BAC C16, and 155 significantly enriched by both BACs (P value < 0.05; Figure 5B). Response to stress was the top biological process enriched by both BACs, as well as cell death and the MAPK cascade (Figure 5C; Table S1). Co-regulated genes by both BACs involved in the response to stress include tribbles homolog 3 (*Trib3*); fibulin 5 (*Fbln5*); solute carrier family 7 member 11 (*Slc7a11*); phosphoenolpyruvate carboxykinase 2, mitochondrial (*Pck2*); asparagine synthetase [glutamine-hydrolyzing] (*Asns*); apolipoprotein E (*Apoe*); and calcium/calmodulin dependent protein kinase II delta (*Camk2d*) (Figure 5D). Of these, all were significantly upregulated except for *Apoe* and *Camk2d*.

A large number of genes involved in integrated stress response was identified by STRING analysis for either BAC (Figure S2), among which a cluster of co-regulated genes by both BACs, including *Trib3, Asns*, and *Slc7a11*, was further identified (Figure 5E). The integrated stress response is an adaptive pathway activated in response to diverse stress stimuli, such as protein homeostasis defects, nutrient deprivation, oxidative stress, and mitochondrial dysfunction, and can lead to cell death in cases of severe stress.[32, 33]

Activating transcription factor 4 (*Atf4*), the main effector of the integrated stress response,[32, 33] was upregulated in response to BAC C12 exposure (LogFC=0.424; adjusted *P* value < 0.05). In addition, *Gpx3* (glutathione peroxidase 3; LogFC = 0.765), *Tnx1* (thioredoxin 1; LogFC=0.567), and *Slc7a11* are also related to response to stress (Figure S1).[34] BAC C16 affected fewer genes involved in the integrated stress response (Figure S1). However, mitochondrial electron transport (specifically cytochrome c to oxygen) was one of the top biological processes enriched in BAC C16-exposed neurospheres (Table 1) and genes encoding for subunits of mitochondrial complex IV were significantly downregulated, including cytochrome c oxidase subunit 6A1 (*Cox6a1*; LogFC = −0.547) and cytochrome c oxidase subunit 7C (*Cox7c*; LogFC = −0.569) (adjusted *P* value < 0.05). Downregulation of genes encoding complex IV subunits may impact the formation and/or stability of complex IV which could impair mitochondrial function.[35] The effect of BAC C16 on genes involved in mitochondrial electron transport is consistent with previous studies that have reported mitochondrial dysfunction in response to BAC exposure.[18, 36, 37]

Finally, of particular relevance to neurodevelopment, neurogenesis was identified as one of the top biological processes enriched in BAC C12-exposed neurospheres (Table 1). Notably, the majority of DEGs involved in neurogenesis were downregulated (adjusted *P* value < 0.05; Figure S3). Among these are the high mobility group family transcription factors *Sox9* (LogFC = −0.554) and *Sox10* (LogFC = −1.262), which are required for the maintenance of the NPC pool;[38, 39] vascular endothelial growth factor A (*Vegf-A*; LogFC = −0.717), which has been shown to increase proliferation and/or decrease apoptosis of NPCs;[40] and noggin (*Nog*; LogFC = −1.524) which encodes a protein that has been shown to regulate neuronal differentiation.[41, 42]

Discussion

In the present study, we aimed to characterize the effects of BAC exposure on neurodevelopment in neurospheres – free floating clusters of NPCs used as an *in vitro* 3-D model for investigating developmental neurotoxicity. Similar to our previous findings, BACs altered cholesterol biosynthesis in neurospheres with BAC C12 being a much more potent inhibitor than BAC C16.[19, 20] However, both BACs impacted neurosphere growth, by inducing apoptosis and inhibiting proliferation, while AY9944 did not, which suggests that inhibition of cholesterol biosynthesis is not the underlying mechanism for the effects on neurosphere growth. To explore alternative mechanisms responsible for the observed phenotype, we carried out a comprehensive transcriptomic analysis, which revealed the integrated stress response as another contributing mechanism to the biological activities of BACs.

The integrated stress response is used by cells to adapt to a variety of stressors, including endoplasmic reticulum (ER) stress, nutrient deficiency, or hypoxia.[32, 33, 43] *Atf4*, the main effector of the integrated stress response, transcriptionally activates *Asns, Slc7a11, and Trib3*.[45] *Asns* converts aspartate and glutamine to asparagine and glutamate in an ATP-dependent reaction and is upregulated in response to amino acid deprivation.[46] *Slc7a11* transports cystine, the oxidized form of cysteine, into cells and releases glutamate into the extracellular space. This gene can be induced by oxidative stress and/or amino acid

deprivation.[34, 47] Finally, *Trib3*, also known as neuronal cell death inducible putative kinase (*Nipk*), is an important mediator of ER stress-related neuronal apoptosis.[48] Trib3 mediates apoptosis through the dephosphorylation of Akt and subsequent activation of Foxo, which leads to the increased expression of PUMA or p53 up-regulated modulator of apoptosis.[49, 50] Upregulation of Trib3 is consistent with the reduced growth and increased apoptosis observed in BAC-exposed neurospheres.

Oxidative stress and mitochondrial dysfunction may play a role in the activation of the integrated stress response as oxidative stress-related genes (such as *Gpx3*, *Tnx1*, and *Slc7a11*) were upregulated and mitochondrial complex IV genes were downregulated in BAC C12- and BAC C16-exposed neurospheres, respectively. Other factors could also contribute to the induction of the integrated stress response in BAC-exposed neurospheres, such as those discussed above. In addition, *Tnx1* has non-redox-related functions, such as regulating lysine methylation.[44] Therefore, it appears that mitochondrial dysfunction, oxidative stress, and dysregulation of protein synthesis all contribute to the activation of the integrated stress response by BACs in neurospheres.[51] Interestingly, mitochondrial dysfunction has also been directly observed by Datta et al. in human corneal epithelial primary cells and osteosarcoma cybrid cells exposed to BAC at low μM concentrations.[36, 37]

Although structure activity differences were not observed in terms of neurosphere growth reduction and apoptosis, BAC C12 altered a greater number of genes than BAC C16, many of which are involved in neurodevelopment. Notably, the majority of DEGs involved in neurogenesis were downregulated by BAC C12 exposure. Cholesterol metabolism is critical for proper neurogenesis. Altered cholesterol biosynthesis has been shown to cause premature differentiation of NPCs.[52, 53] Additionally, Francis *et al.* demonstrated that accumulation of the cholesterol precursor, 7-DHC, is responsible for this phenomenon.[53] Although BAC C12 exposure led to 7-DHC accumulation and downregulation of genes involved in neurogenesis, effects indicative of premature differentiation were not observed with the current experimental paradigm. Therefore, further studies using alternative strategies are needed to examine defects in neurogenesis related to altered cholesterol biosynthesis by BAC C12.

In conclusion, we have demonstrated that BACs potently reduce neurosphere growth through increased apoptosis and inhibited proliferation at nM concentrations, and that these activities of BACs are associated with induction of the integrated stress response rather than inhibition of cholesterol biosynthesis, suggesting a diverse range of biological activities exerted by BACs.

Supplementary Material

Refer to Web version on PubMed Central for supplementary material.

Acknowledgements

The work was supported by grants from the National Institutes of Health: R01HD092659, the University of Washington (UW) Environmental Pathology/Toxicology Training Program (T32ES007032), and the UW Interdisciplinary Center for Exposures, Diseases, Genomics and Environment (UW EDGE) (P30ES007033), as well as start-up funds from the Department of Medicinal Chemistry at the UW.

References

1. Kim M; Weigand MR; Oh S; Hatt JK; Krishnan R; Tezel U; Pavlostathis SG; Konstantinidis KT, Widely used benzalkonium chloride disinfectants can promote antibiotic resistance. Applied and Environmental Microbiology 2018, 84 (17).
2. Gilbert P; Moore LE, Cationic antiseptics: diversity of action under a common epithet. J. Appl. Microbiol 2005, 99 (4), 703–15. [PubMed: 16162221]
3. US FDA, Safety and Effectiveness of Health Care Antiseptics; Topical Antimicrobial Drug Products for Over-the-Counter Human Use; Proposed Amendment of the Tentative Final Monograph; Reopening of Administrative Record. Federal Register 2015, 21 CFR Part 310, 80 (84), 25165–25205.
4. US FDA, Safety and Effectiveness of Consumer Antiseptics; Topical Antimicrobial Drug Products for Over-the-Counter Human Use; Proposed Amendment of the Tentative Final Monograph; Reopening of Administrative Record Federal Register 2016, 21 CFR Part 310, 81 (126), 42911–42937.
5. Gonzalez M; Jégu J; Kopferschmitt MC; Donnay C; Hedelin G; Matzinger F; Velten M; Guilloux L; Cantineau A; de Blay F, Asthma among workers in healthcare settings: role of disinfection with quaternary ammonium compounds. Clin Exp Allergy 2014, 44 (3), 393–406. [PubMed: 24128009]
6. Purohit A; Kopferschmitt-Kubler MC; Moreau C; Popin E; Blaumeiser M; Pauli G, Quaternary ammonium compounds and occupational asthma. Int. Arch. Occup. Environ. Health 2000, 73 (6), 423–7. [PubMed: 11007347]
7. Paris C; Ngatchou-Wandji J; Luc A; McNamee R; Bensefa-Colas L; Larabi L; Telle-Lamberton M; Herin F; Bergeret A; Bonneterre V; Brochard P; Choudat D; Dupas D; Garnier R; Pairon JC; Agius RM; Ameille J; Members of the RP, Work-related asthma in France: recent trends for the period 2001–2009. Occup Environ Med 2012, 69 (6), 391–7. [PubMed: 22383588]
8. Vandenplas O; D'Alpaos V; Evrard G; Jamart J; Thimpont J; Huaux F; Renauld JC, Asthma related to cleaning agents: a clinical insight. BMJ Open 2013, 3 (9), e003568.
9. Baudouin C; Labbe A; Liang H; Pauly A; Brignole-Baudouin F, Preservatives in eyedrops: the good, the bad and the ugly. Prog. Retin. Eye Res 2010, 29 (4), 312–34. [PubMed: 20302969]
10. Robinson AJ; Foster RS; Halbert AR; King E; Orchard D, Granular parakeratosis induced by benzalkonium chloride exposure from laundry rinse aids. Australas J Dermatol 2017, 58 (3), e138–e140. [PubMed: 27641714]
11. Herman JR; Bass P, Enteric neuronal ablation: structure-activity relationship in a series of alkyldimethylbenzylammonium chlorides. Fundam. Appl. Toxicol 1989, 13 (3), 576–84. [PubMed: 2612790]
12. Sarkar J; Chaudhary S; Namavari A; Ozturk O; Chang JH; Yco L; Sonawane S; Khanolkar V; Hallak J; Jain S, Corneal neurotoxicity due to topical benzalkonium chloride. Invest. Ophthalmol. Vis. Sci 2012, 53 (4), 1792–802. [PubMed: 22410563]
13. Melin VE; Potineni H; Hunt P; Griswold J; Siems B; Werre SR; Hrubec TC, Exposure to common quaternary ammonium disinfectants decreases fertility in mice. Reprod. Toxicol 2014, 50, 163–70. [PubMed: 25483128]
14. Hrubec TC; Melin VE; Shea CS; Ferguson EE; Garofola C; Repine CM; Chapman TW; Patel HR; Razvi RM; Sugrue JE; Potineni H; Magnin-Bissel G; Hunt PA, Ambient and Dosed Exposure to Quaternary Ammonium Disinfectants Causes Neural Tube Defects in Rodents. Birth Defects Research 2017, 109 (14), 1166–1178. [PubMed: 28618200]
15. Hirata H; Tomita K; Bessho Y; Kageyama R, Hes1 and Hes3 regulate maintenance of the isthmic organizer and development of the mid/hindbrain. EMBO Journal 2001, 20 (16), 4454–4466.
16. Ishibashi M; Ang SL; Shiota K; Nakanishi S; Kageyama R; Guillemot F, Targeted disruption of mammalian hairy and Enhancer of split homolog-1 (HES-1) leads to up-regulation of neural helix-loop-helix factors, premature neurogenesis, and severe neural tube defects. Genes and Development 1995, 9 (24), 3136–3148. [PubMed: 8543157]
17. Zhong W; Jiang MM; Schonemann MD; Meneses JJ; Pedersen RA; Jan LY; Jan YN, Mouse numb is an essential gene involved in cortical neurogenesis. Proceedings of the National Academy of Sciences of the United States of America 2000, 97 (12), 6844–6849. [PubMed: 10841580]

18. Ryu O; Park BK; Bang M; Cho KS; Lee SH; Gonzales ELT; Yang SM; Kim S; Eun PH; Lee JY; Kim KB; Shin CY; Kwon KJ, Effects of several cosmetic preservatives on ros-dependenapoptosis of rat neural progenitor cells. Biomolecules and Therapeutics 2018, 26 (6), 608–615. [PubMed: 29429147]
19. Herron J; Reese R; Tallman KA; Narayanaswamy R; Porter NA; Xu L, Identification of Environmental Quaternary Ammonium Compounds as Direct Inhibitors of Cholesterol Biosynthesis. Toxicol. Sci 2016, 151 (2), 261–270. [PubMed: 26919959]
20. Herron JM; Hines KM; Tomita H; Seguin RP; Cui JY; Xu L, Multiomics investigation reveals benzalkonium chloride disinfectants alter sterol and lipid homeostasis in the mouse neonatal brain. Toxicol. Sci 2019, 171, 32–45.
21. Porter JA; Young KE; Beachy PA, Cholesterol modification of hedgehog signaling proteins in animal development. Science 1996, 274 (5285), 255–9. [PubMed: 8824192]
22. Komada M; Saitsu H; Kinboshi M; Miura T; Shiota K; Ishibashi M, Hedgehog signaling is involved in development of the neocortex. Development 2008, 135 (16), 2717–2727. [PubMed: 18614579]
23. Koudinov AR; Koudinova NV, Essential role for cholesterol in synaptic plasticity and neuronal degeneration. The FASEB Journal 2001, 15 (10), 1858–1860. [PubMed: 11481254]
24. Mauch DH; Nägier K; Schumacher S; Göritz C; Müller EC; Otto A; Pfrieger FW, CNS synaptogenesis promoted by glia-derived cholesterol. Science 2001, 294 (5545), 1354–1357. [PubMed: 11701931]
25. Saher G; Brugger B; Lappe-Siefke C; Mobius W; Tozawa R; Wehr MC; Wieland F; Ishibashi S; Nave KA, High cholesterol level is essential for myelin membrane growth. Nat. Neurosci 2005, 8 (4), 468–75. [PubMed: 15793579]
26. Chen J; Costa LG; Guizzetti M, Retinoic acid isomers up-regulate ATP binding cassette A1 and G1 and cholesterol efflux in rat astrocytes: Implications for their therapeutic and teratogenic effects. Journal of Pharmacology and Experimental Therapeutics 2011, 338 (3), 870–878.
27. Zhou C; Chen J; Zhang X; Costa LG; Guizzetti M, Prenatal ethanol exposure up-regulates the cholesterol transporters ATP-binding cassette A1 and G1 and reduces cholesterol levels in the developing rat brain. Alcohol and Alcoholism 2014, 49 (6), 626–634. [PubMed: 25081040]
28. Fritsche E; Gassmann K; Schreiber T, Neurospheres as a model for developmental neurotoxicity testing. Methods in Molecular Biology 2011, 758, 99–114. [PubMed: 21815061]
29. Moors M; Rockel Thomas D; Abel J; Cline Jason E; Gassmann K; Schreiber T; Schuwald J; Weinmann N; Fritsche E, Human Neurospheres as Three-Dimensional Cellular Systems for Developmental Neurotoxicity Testing. Environmental Health Perspectives 2009, 117 (7), 1131–1138. [PubMed: 19654924]
30. Xu L; Korade Z; Rosado DA; Liu W; Lamberson CR; Porter NA, An oxysterol biomarker for 7-dehydrocholesterol oxidation in cell/mouse models for Smith-Lemli-Opitz syndrome. J. Lipid Res 2011, 52 (6), 1222–1233. [PubMed: 21402677]
31. Herron J; Hines KM; Xu L, Assessment of Altered Cholesterol Homeostasis by Xenobiotics Using Ultra-High Performance Liquid Chromatography-Tandem Mass Spectrometry. Curr Protoc Toxicol 2018, 78 (1), e65. [PubMed: 30320450]
32. Pakos-Zebrucka K; Koryga I; Mnich K; Ljujic M; Samali A; Gorman AM, The integrated stress response. EMBO Rep 2016, 17 (10), 1374–1395. [PubMed: 27629041]
33. Costa-Mattioli M; Walter P, The integrated stress response: From mechanism to disease. Science 2020, 368 (6489).
34. Lewerenz J; Hewett SJ; Huang Y; Lambros M; Gout PW; Kalivas PW; Massie A; Smolders I; Methner A; Pergande M; Smith SB; Ganapathy V; Maher P, The Cystine/Glutamate Antiporter System xc− in Health and Disease: From Molecular Mechanisms to Novel Therapeutic Opportunities. Antioxidants & Redox Signaling 2012, 18 (5), 522–555. [PubMed: 22667998]
35. Poché RA; Zhang M; Rueda EM; Tong X; McElwee ML; Wong L; Hsu C-W; Dejosez M; Burns AR; Fox DA; Martin JF; Zwaka TP; Dickinson ME, RONIN Is an Essential Transcriptional Regulator of Genes Required for Mitochondrial Function in the Developing Retina. Cell reports 2016, 14 (7), 1684–1697. [PubMed: 26876175]

36. Datta S; Baudouin C; Brignole-Baudouin F; Denoyer A; Cortopassi GA, The Eye Drop Preservative Benzalkonium Chloride Potently Induces Mitochondrial Dysfunction and Preferentially Affects LHON Mutant Cells. Invest. Ophthalmol. Vis. Sci 2017, 58 (4), 2406–2412. [PubMed: 28444329]
37. Datta S; He G; Tomilov A; Sahdeo S; Denison MS; Cortopassi G, In Vitro Evaluation of Mitochondrial Function and Estrogen Signaling in Cell Lines Exposed to the Antiseptic Cetylpyridinium Chloride. Environ. Health Perspect 2017, 125 (8), 087015. [PubMed: 28885978]
38. Kim J; Lo L; Dormand E; Anderson DJ, SOX10 maintains multipotency and inhibits neuronal differentiation of neural crest stem cells. Neuron 2003, 38 (1), 17–31. [PubMed: 12691661]
39. Vong KI; Leung CKY; Behringer RR; Kwan KM, Sox9 is critical for suppression of neurogenesis but not initiation of gliogenesis in the cerebellum. Molecular Brain 2015, 8 (1).
40. Mackenzie F; Ruhrberg C, Diverse roles for VEGF-A in the nervous system. Development 2012, 139 (8), 1371–80. [PubMed: 22434866]
41. Li W; LoTurco JJ, Noggin is a negative regulator of neuronal differentiation in developing neocortex. Developmental Neuroscience 2000, 22 (1–2), 68–73. [PubMed: 10657699]
42. Lim DA; Tramontin AD; Trevejo JM; Herrera DG; García-Verdugo JM; Alvarez-Buylla A, Noggin antagonizes BMP signaling to create a niche for adult neurogenesis. Neuron 2000, 28 (3), 713–726. [PubMed: 11163261]
43. Wang SF; Wung CH; Chen MS; Chen CF; Yin PH; Yeh TS; Chang YL; Chou YC; Hung HH; Lee HC, Activated Integrated Stress Response Induced by Salubrinal Promotes Cisplatin Resistance in Human Gastric Cancer Cells via Enhanced xCT Expression and Glutathione Biosynthesis. International journal of molecular sciences 2018, 19 (11).
44. Liu T; Wu C; Jain MR; Nagarajan N; Yan L; Dai H; Cui C; Baykal A; Pan S; Ago T; Sadoshima J; Li H, Master redox regulator Trx1 upregulates SMYD1 & modulates lysine methylation. Biochim Biophys Acta 2015, 1854 (12), 1816–1822. [PubMed: 26410624]
45. Evstafieva AG; Garaeva AA; Khutornenko AA; Klepikova AV; Logacheva MD; Penin AA; Novakovsky GE; Kovaleva IE; Chumakov PM, A sustained deficiency of mitochondrial respiratory complex III induces an apoptotic cell death through the p53-mediated inhibition of pro-survival activities of the activating transcription factor 4. Cell Death and Disease 2014, 5 (11).
46. Balasubramanian MN; Butterworth EA; Kilberg MS, Asparagine synthetase: regulation by cell stress and involvement in tumor biology. Am J Physiol Endocrinol Metab 2013, 304 (8), E789–99. [PubMed: 23403946]
47. Sato H; Nomura S; Maebara K; Sato K; Tamba M; Bannai S, Transcriptional control of cystine/glutamate transporter gene by amino acid deprivation. Biochem Biophys Res Commun 2004, 325 (1), 109–16. [PubMed: 15522208]
48. Zhang J; Han Y; Zhao Y; Li Q; Jin H; Qin J, Inhibition of TRIB3 protects against neurotoxic injury induced by kainic acid in rats. Frontiers in Pharmacology 2019, 10 (5).
49. Saleem S; Biswas SC, Tribbles pseudokinase 3 induces both apoptosis and autophagy in amyloid-$β$-induced neuronal death. Journal of Biological Chemistry 2017, 292 (7), 2571–2585.
50. Zou CG; Cao XZ; Zhao YS; Gao SY; Li SD; Liu XY; Zhang Y; Zhang KQ, The molecular mechanism of endoplasmic reticulum stress-induced apoptosis in PC-12 neuronal cells: The protective effect of insulin-like growth factor I. Endocrinology 2009, 150 (1), 277–285. [PubMed: 18801901]
51. Silva JM; Wong A; Carelli V; Cortopassi GA, Inhibition of mitochondrial function induces an integrated stress response in oligodendroglia. Neurobiology of disease 2009, 34 (2), 357–365. [PubMed: 19233273]
52. Driver AM; Kratz LE; Kelley RI; Stottmann RW, Altered cholesterol biosynthesis causes precocious neurogenesis in the developing mouse forebrain. Neurobiology of Disease 2016, 91, 69–82. [PubMed: 26921468]
53. Francis KR; Ton AN; Xin Y; O'Halloran PE; Wassif CA; Malik N; Williams IM; Cluzeau CV; Trivedi NS; Pavan WJ; Cho W; Westphal H; Porter FD, Modeling Smith-Lemli-Opitz syndrome with induced pluripotent stem cells reveals a causal role for Wnt/β-catenin defects in neuronal cholesterol synthesis phenotypes. Nature Medicine 2016, 22 (4), 388–396.

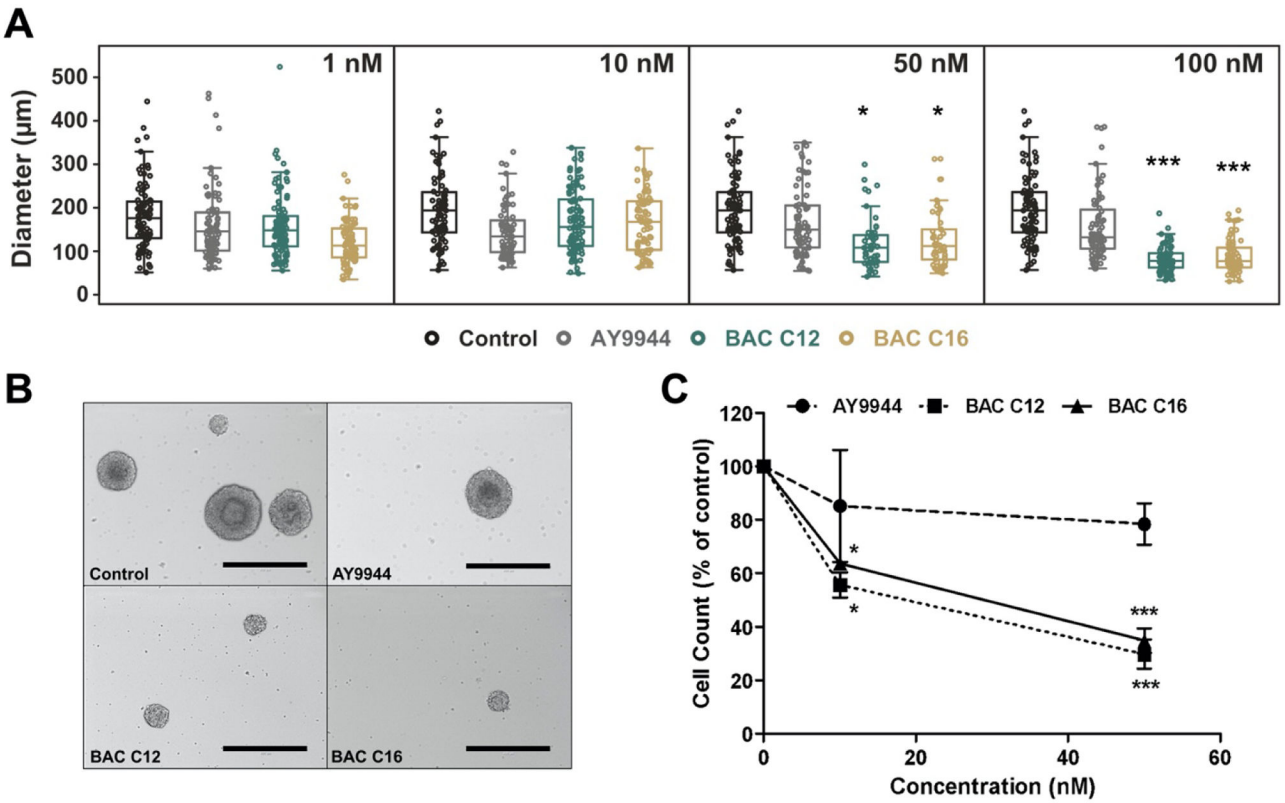

Figure 1. BACs reduce neurosphere growth.

(A) Size distribution of neurospheres exposed to vehicle control, AY9944 (positive control), BAC C12, or BAC C16 at a concentration of 1, 10, 50, and 100 nM from DIV 4 to DIV 7. (B) Representative brightfield images of neurospheres exposed to a concentration of 50 nM from DIV 4 to DIV 7 (scale bar: 400 µm). (C) Number of neural progenitor cells from dissociated neurospheres exposed to vehicle control (0 nM), AY9944, BAC C12, or BAC C16 at 10 and 50 nM from DIV 4 to DIV 7. N = 4 biological replicates per condition. Adjusted *P* value: *, $P < 0.05$; **, $P < 0.01$; ***, $P < 0.001$.

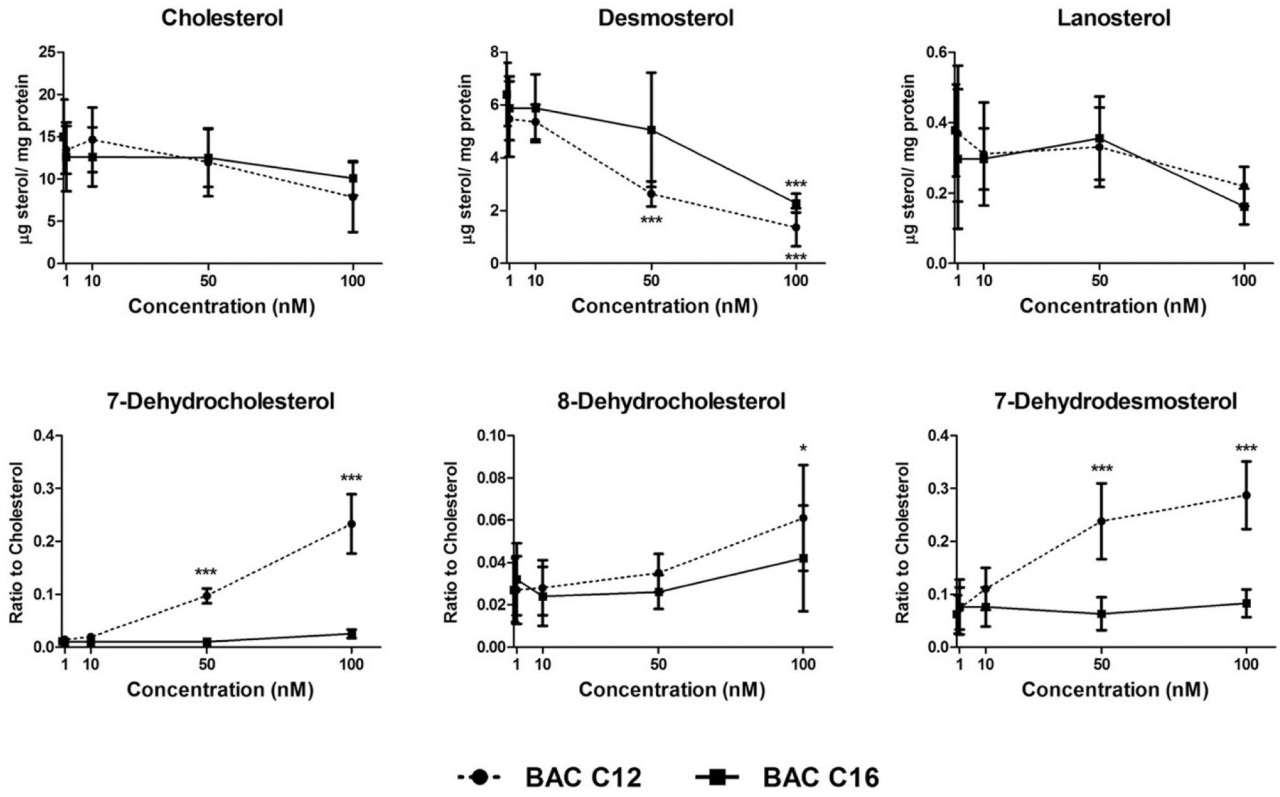

Figure 2. BACs alter cholesterol biosynthesis.

Neurospheres exposed to vehicle control (0 nM), BAC C12 or BAC C16 at 1, 10, 50, and 100 nM from DIV 4 to DIV 7 show alterations in levels of sterols in the post-squalene cholesterol biosynthetic pathway. N = 4 biological replicates per condition. Adjusted *P* value: *, $P < 0.05$; **, $P < 0.01$; ***, $P < 0.001$.

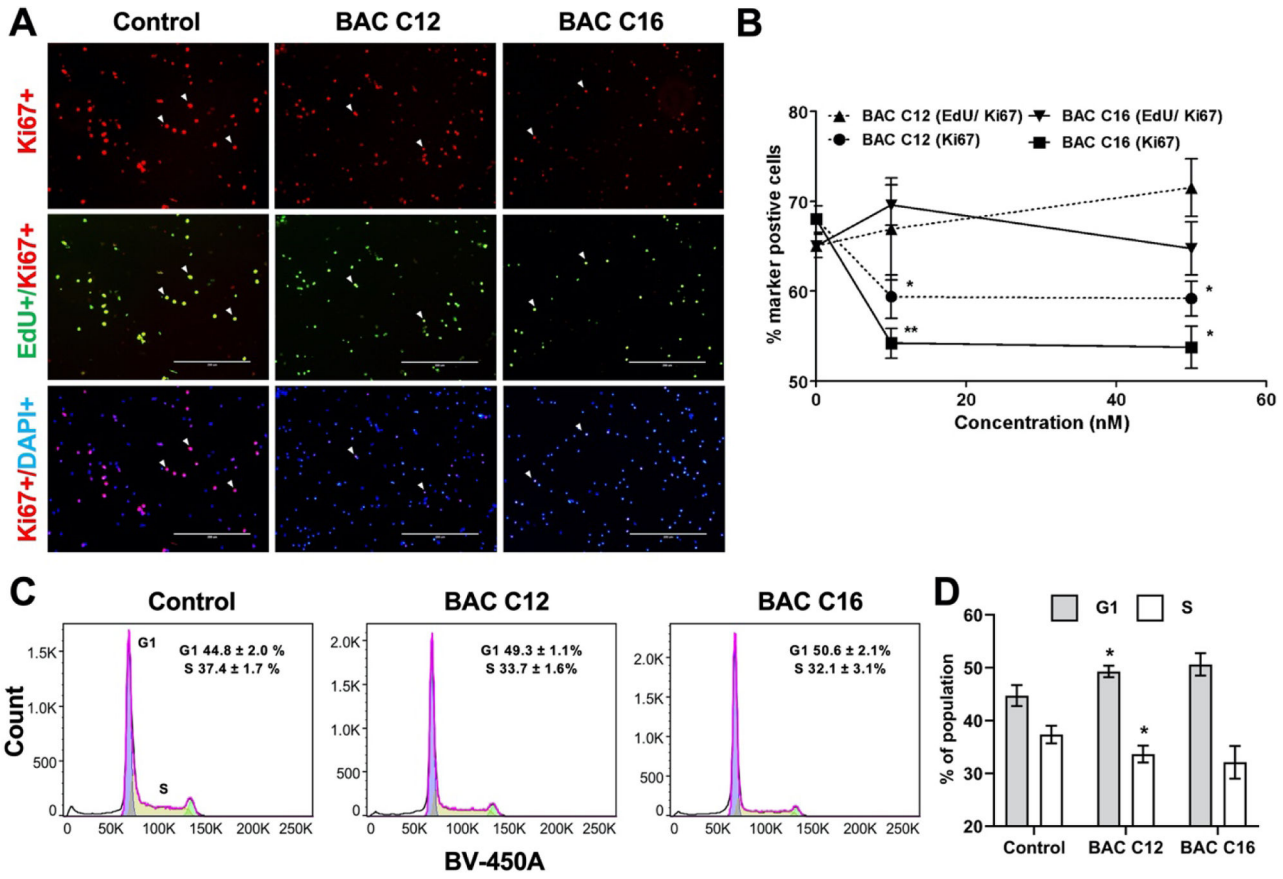

Figure 3. BACs decrease pool of proliferative NPCs.

(A) Immunocytochemistry for Ki67 (red) and EdU (green), counterstained with DAPI (blue) of NPCs from dissociated neurospheres exposed to vehicle control (0 nM) or 50 nM of BAC C12 or BAC C16 from DIV 4 to DIV 7. (B) Quantification of proliferation rate (Edu/Ki67) and percentage of proliferative cells (Ki67) cells. Adjusted *P* value: *, $P < 0.05$; **, $P < 0.01$; ***, $P < 0.001$. (C) Cell cycle analysis of nuclei isolated from dissociated neurospheres exposed to vehicle control or 50 nM of BAC C12 or BAC C16 from DIV 4 to DIV 5. (D) Quantitation of population of cells in G1 or S phase in (C); *, $P < 0.05$ relative to Control. N = 4 biological replicates per condition.

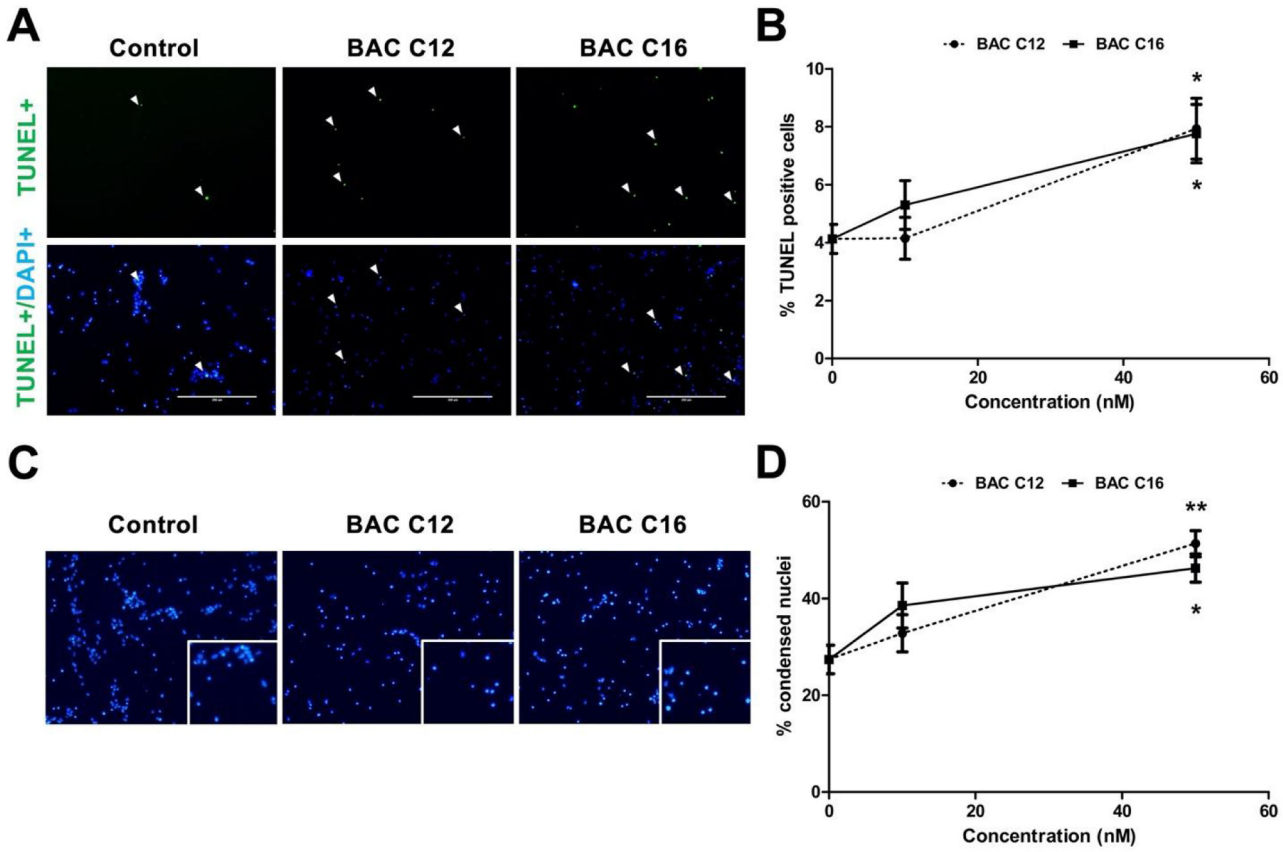

Figure 4. BACs induce apoptosis of NPCs.

(A) Immunocytochemistry for TUNEL (green) counterstained with DAPI (blue) of NPCs exposed to vehicle control (0 nM) or 50 nM of BAC C12 or BAC C16 from DIV 4 to DIV 7. (B) Quantification of percentage of TUNEL-positive NPCs. (C) DAPI-stained nuclei for each exposure group. Enlarged image in bottom right corner shows condensed nuclei. (D) Quantification of percentage of condensed nuclei. N = 4 biological replicates per condition. Adjusted *P* value: *, $P < 0.05$; **, $P < 0.01$; ***, $P < 0.001$.

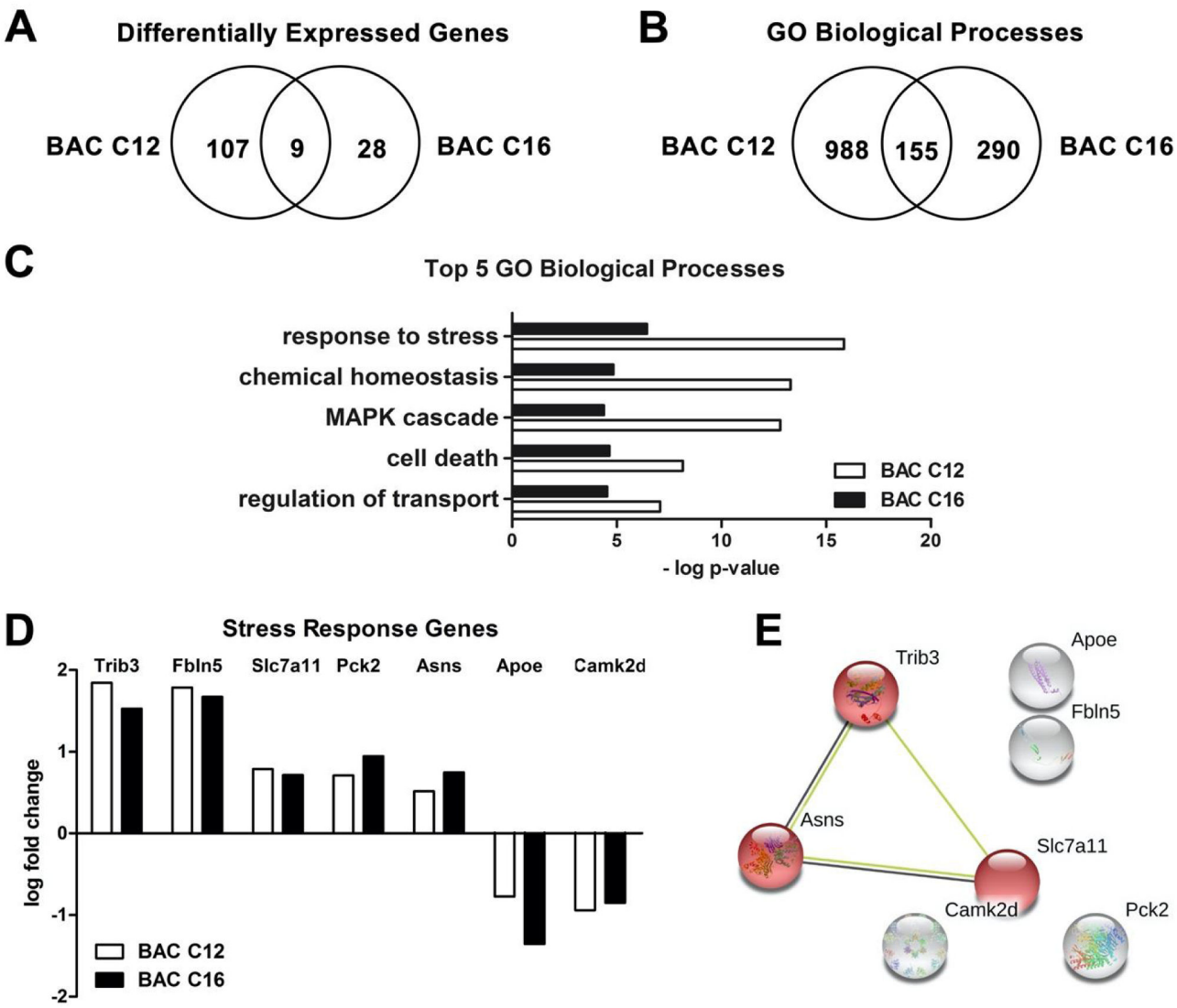

Figure 5. Transcriptome analysis indicates a stress response in BAC-exposed neurospheres.

(A) Venn diagram of DEGs from neurospheres exposed to 50 nM BAC C12 or BAC C16 from DIV 4 to DIV 5. (B) Venn diagram of GO biological processes affected by either or both BACs. (C) Top 5 significantly enriched GO biological processes. (D) Co-regulated DEGs involved in the "response to stress" biological process. (E) STRING analysis of DEGs co-regulated by both BACs. Red indicates genes involved in the integrated stress response. N = 3 biological replicates per condition. Adjusted *P* values for all DEGs are < 0.05.

Table 1.

Top 10 biological processes altered by BAC C12 and BAC C16.

	Identifier	Name	# DEGs	# Total	−log *P* value
BAC C12 vs. Control	GO:0061564	axon development	20	384	30.1
	GO:0007154	cell communication	63	3287	29.6
	GO:0023052	signaling	62	3249	28.7
	GO:0050896	response to stimulus	77	4701	28.0
	GO:0097485	neuron projection guidance	12	168	23.4
	GO:0022008	neurogenesis	33	1275	23.1
	GO:0040011	locomotion	31	1153	22.9
	GO: 0048869	cellular developmental process	51	2703	21.5
	GO:0048731	system development	54	2963	21.4
	GO:0009653	anatomical structure morphogenesis	39	1781	21.1
BAC C16 vs. Control	GO:0043603	cellular amide metabolic process	10	789	14.8
	GO:0043604	amide biosynthetic process	8	606	12.4
	GO:0044281	small molecule metabolic process	11	1178	12.3
	GO:0006123	mitochondrial electron transport, cytochrome c to oxygen	2	8	12.2
	GO:0097688	glutamate receptor clustering	2	9	11.9
	GO:1901617	organic hydroxy compound biosynthetic process	4	132	11.1
	GO:0045833	negative regulation of lipid metabolic process	3	55	11.1
	GO:0006641	triglyceride metabolic process	3	58	10.9
	GO:0072578	neurotransmitter-gated ion channel clustering	2	13	10.8
	GO:0019752	carboxylic acid metabolic process	7	575	10.2